Journal of the Korean Ceramic Society
Vol. 38, No.1 pp. 100~105 2001

Pt Doping Mechanism of Vanadium Oxide Cathode Film Grown on ITO Glass for Thin Film Battery

Han-Ki Kim*,, Tae-Yeon Seong**, Eun Jeong Jeon*, Won Il Cho* and Young Soo Yoon*,****

**Thin Film Technology Research Center &, Battery and Fuel Cell Research Center Korea Institute of Science and Technology (KIST), Seoul, 136-791, Korea*
***Department of Materials Science and Engineering, and Center for Electronic Materials Research, Kwangju Institute of Science and Technology (K-JIST), Kwangju, 500-712, Korea*
(Received November 27, 2000)

An all solid-state thin film battery (TFB) was fabricated by growing, undoped and Pt-doped vanadium oxide cathode film (V_2O_5) on In_2O_3:Sn coated glass, respectively. Room temperature charge-discharge measurements based on Li/Lipon/V_2O_5 full-cell structure with a constant current clearly shows that the Pt-doped V_2O_5 cathode film is superior, in terms of cyclibility. X-ray diffraction (XRD) results indicate that the Pt doping process induces a more random amorphous structure than an undoped V_2O_5 film. In addition to its modified structure, the Pt-doped V_2O_5 film has a smoother surface than the undoped sample. Compared to an undoped V_2O_5 film, the Pt doped V_2O_5 cathode film has a higher electron conductivity. We hypothesize that the addition of Pt alters electrochemical performance in a manner of making more random amorphous structure and gives an excess electron by replacing the V^{+5}. Possible mechanisms are discussed for the observed Pt doping effect on structural and electrochemical properties of vanadium oxide cathode films, which are grown on In_2O_3:Sn coated glass.

Key words: Thin film battery, V_2O_5, Amorphous, Pt-doping, Conductivity

1. Introduction

There is considerable interest in the power sources for microelectronics and, as a result, it has promoted large research efforts in thin film battery (TFB) technology. Because a TFB has a unique advantage, in that it can be incorporated into the same integrated circuit with other electronic elements, it has great potential for use in areas, such as microelectronic mechanical systems (MEMS), smart cards, on-chip power sources and portable electronic devices. To enhance TFB performance, the development of a high quality cathode film, which has high energy density, good reversibility, and thermal stability is a critical issue. Therefore a variety of cathode films, such as V_2O_5, LiV_2O_5, $LiMn_2O_4$, and $LiCoO_2$ have been reported as good candidates for use as a cathode for a thin film battery (TFB).[1-4] However, crystalline cathodes can result in poor contacts with the thin-film solid electrolyte and fast ions are largely impeded at phase boundaries. In addition, the Li intercalation into the crystalline cathode results in a phase transformation of cathode film. To solve this problem, many researchers have investigated amorphous cathode film, but little has been reported to date with respect to amorphous cathode films, which are used in TFBs. Of the many possible cathode materials, the amorphous vanadium oxide (V_2O_5) film has been attracted attention as a promising candidate for use as a cathode material for TFB, due to its unique isotropic structure and faster ion channels over those of crystalline films.[5,6] Bates *et al.* reported on amorphous V_2O_5 films with a charge capacity of 1.5 Li atoms per vanadium oxide.[7] Park *et al.* also reported improved charging capacities for a V_2O_5 xerogel film, which was used as intercalation hosts for lithium.[8] In order to improve the electrical properties of cathode film, it is desirable to employ a doping process, which represents conventional method in semiconductor technology. Coustier *et al.*, who investigated the Cu and Ag doped vanadium oxide as host materials for Li intercaltion, suggested that the electronic conductivity of V_2O_5 was increased by two to three magnitudes by means of Cu and Ag doping.[9] Although some researchers have used amorphous V_2O_5 films as a cathode film, there are no reports concerning doping effects on such materials.

In this paper, we report the Pt doping effect and relate to the electrochemical, structural, electrical and optical properties of amorphous vanadium oxide films grown on ITO glasses by rf magnetron sputtering. Based on these results, a possible mechanism for enhancing TFB performance by Pt doping is proposed.

2. Experimental

The V_2O_5 cathode film was deposited on a ITO (In_2O_3:Sn)/

coring glass substrate by means of a specially designed dual target magnetron sputtering system using a pure vanadium metal target. The ITO film, which was grown on corning glass acts as a current collector to diminish the potential drop between the electrode and the collector, and to apply uniform voltage to the electrode. The V_2O_5 electrode films were grown on ITO current collectors by direct current (dc) reactive sputtering with 600W dc power at room temperature. Simultaneously, the Pt was doped into the V_2O_5 film by co-sputtering the high purity Pt metal target with 10W radio frequency (rf) power. The base pressure in the chamber was maintained at 5×10^{-6} Torr and the working pressure was maintained at 5 mTorr, respectively. The extent of Pt incorporation into the V_2O_5 cathode film was characterized by Auger electron spectroscopy (AES) depth profile using a PHI 670 Auger microscope with an electron beam of 10 keV and 0.0236 μA. After the deposition of the V_2O_5 film deposition, a LiPON ($Li_{2.18}PO_{3.1}N_{0.7}$) electrolyte film was deposited onto the as-deposited the V_2O_5 electrode film by an rf sputtering method, in order to compare electrochemical properties of both undoped and Pt-doped V_2O_5 cathode film as a shape of all solid-state TFB. Subsequently, the Li anode metal was evaporated on the LiPON by electron beam evaporation. Fig. 1 shows the schematic feature of an all solid-state TFB. Room temperature charge-discharge property based on all solid-state full-cell, which is shown in Fig. 1, with a constant current of 20 μA/cm^2 was measured by a cycler (Wonatech com. WBCS300). The structure properties of both the undoped and Pt-doped V_2O_5 films were examined by x-ray diffraction (XRD:Rigaku, 20B diffractometer with CuK_α radiation) measurements. Scanning electron microscopy (SEM: HITACHI, S-4100) and atomic force microscopy (AFM: PSIA) were employed to compare the surface morphology of both the undoped and the Pt-doped sample. The electrical properties of both the undoped and the Pt-doped V_2O_5 films were measured by Hall effect measurement(Bio-Rad Co., UK) with van der Pouw geometry. To explain the Pt doping effect using a band gap model, the optical-absorption spectra of both the undoped and the Pt-doped V_2O_5 films were measured in the wavelength range 300-800 nm at room temperature. Absorption spectra were recorded on Model ARC Spectra Pro 300I. A blank ITO/corning glass substrate was used in the reference beam to eliminate the substrate absorption cut-off and to compensate for any glass impurities. From these electrical and optical properties, we suggest the possible mechanism, which describe the Pt doping effect on V_2O_5 films.

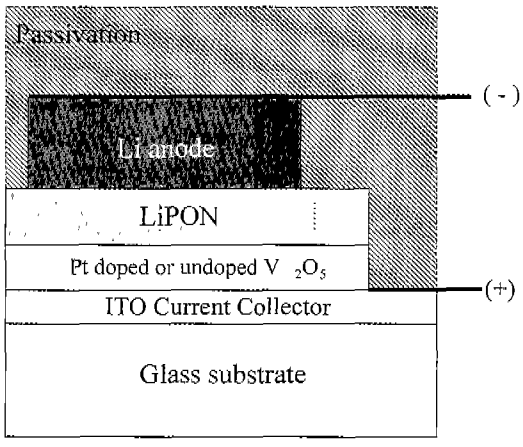

Fig. 1. Schematic cross section of an all- solid- state thin film battery (TFB) on an ITO coated glass substrate.

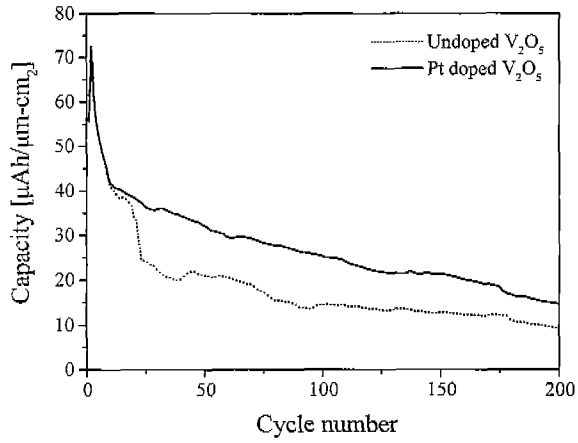

Fig. 2. The discharge capacities of the undoped and Pt-doped V_2O_5 films (cycled between 2.2 and 3.2 V) as a function of cycle number. It can be clearly seen that the addition of Pt leads to an improvement in the cycling behaviour of the films.

3. Results and Discussion

Fig. 2 shows the discharge capacities for the undoped and the Pt-doped V_2O_5 films. It is noteworthy that the 10W Pt doped V_2O_5 films clearly show a more improved cyclibility than the undoped V_2O_5 sample. The initial large capacity fade of both samples is thought to be caused by Li entrapment during Li intercalation. The different cycle properties between undoped and Pt-doped V_2O_5 films probably relate to the V_2O_5 film structure modification caused by the Pt doping process.

Fig. 3 shows the 1st ~ 4th discharge curves for undoped and Pt-doped V_2O_5 films. Even though the undoped V_2O_5 film shows a higher open circuit voltage than the Pt-doped V_2O_5 film, a plateau appears in the range of 3.2 V. This plateau indicates that undoped V_2O_5 film undergoes a phase transformation as a result of Li intercalation. In the case of Pt doped V_2O_5 film, it shows perfect amorphous characteristics with no plateau, as shown in Fig. 3 (b). In a previous report, we already showed that an amorphous vanadium oxide film without short-range order could be obtained by the Pt doping process.[10-11] Therefore, it was thought that the discharge curve characteristics of the V_2O_5 film could be changed via the structural modification of the cathode film, which was obtained by a Pt co-sputtering process.

Fig. 4 shows the AES depth profiles of both the undoped and 10 W rf powers Pt doped V_2O_5 films. For the undoped sample, the AES result reveals a uniform distribution of

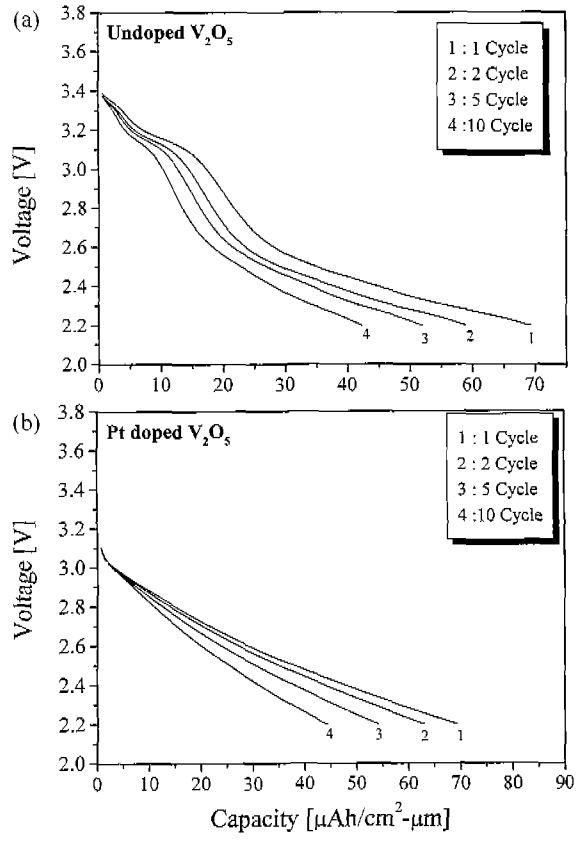

Fig. 3. Discharge curves for (a) the undoped and (b) Pt-doped films prepared at a rf power of 10 W.

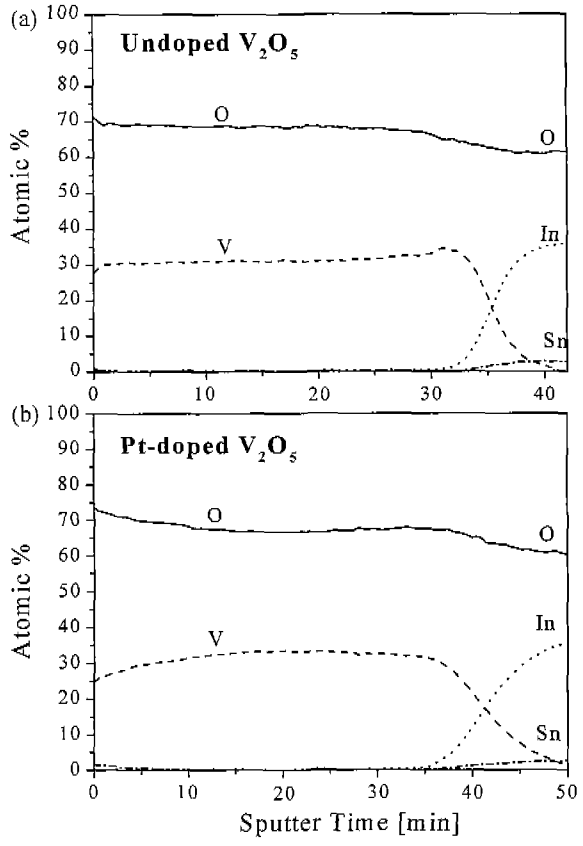

Fig. 4. AES depth profiles of (a) undoped V_2O_5 films and (b) film doped at an rf power of 10 W. A uniform distribution of vanadium and oxygen exists in both the undoped and the Pt-doped sample. These results indicate that the Pt co-sputtered V_2O_5 film can be legitimately characterized as Pt-doped V_2O_5.

vanadium and oxygen, Fig. 4(a). For the 10 W-doped film, it shows results, which are similar to that of undoped V_2O_5 films. These results indicate that the Pt co-sputtered V_2O_5 film can be legitimately characterized as Pt-doped V_2O_5. A compositional analysis was performed by Rutherford back-scattering spectrometry (RBS), which indicate that a typical film consisted of $Pt_{0.01}V_2O_5$ (Detailed results not shown here).

To characterize the doping effect on the microstructure of V_2O_5 films, the x-ray diffraction examination was employed. Fig. 5 shows the XRD plots of the V_2O_5 films. The XRD plot of the undoped film reveals diffraction peaks, which are charateristic of crystalline V_2O_5 (2θ = 36.0° (211) and 2θ = 51.0° (020)). In addition, there is a broad extra peak, which is identified to be amorphous (a) V_2O_5. This XRD feature indicates that the undoped V_2O_5 film is not completely amorphous, but includes some microcrystalline phases. A similar structure was observed in V_2O_5 xerogel films.[12, 13] Based on the XRD results, Aldebert *et al.*,[12] and Legendre and Livage[13] concluded that the spin-coated V_2O_5 films were amorphous with short-range order which consists of self-aligned ribbon-like fibers. For the 10 W-doped film, however, only a broad amorphous V_2O_5 peak (2θ = 26.7°) is apparent. In order to clarify the structure of the amorphous phase, the sample was further investigated by means of x-ray q-rocking. The q-rocking plot exhibited a broad peak, implying that the V_2O_5 phase is amorphous. Based on these XRD results, it is clear that the structural modification take place by Pt-doping process. The origin of the difference in cycle performance between undoped and Pt doped V_2O_5 films can be attributed to the extent of disorder in the cathode film. Another reason for this difference in cycle performance can be attributed to the volume buffering effects due to the presence of Pt crystallites. In other words, an amorphous V_2O_5 cathodes could undergo volume expansion during a Li insertion-extraction process. The dispersed Pt microcrystallites could suppress the volume expansion (which represents a possible factor for the degradation of the reversibility of Li intercalation), consequently leading to improved performance.

Fig. 6 shows the cross sectional SEM images of both the undoped (a) and 10 W rf power Pt doped V_2O_5 films (b). For the undoped sample, a rough surface and a less dense film structure is observed, compared to that of the Pt-doped V_2O_5 films. However, the cross sectional SEM image of the Pt-doped V_2O_5 film shows that it was efficiently deposited on ITO film without any defects such as holes and cracks, as shown in Fig. 6 (b). In addition, the Pt-doped V_2O_5 film reveals a fairly smooth surface, which is very important fac-

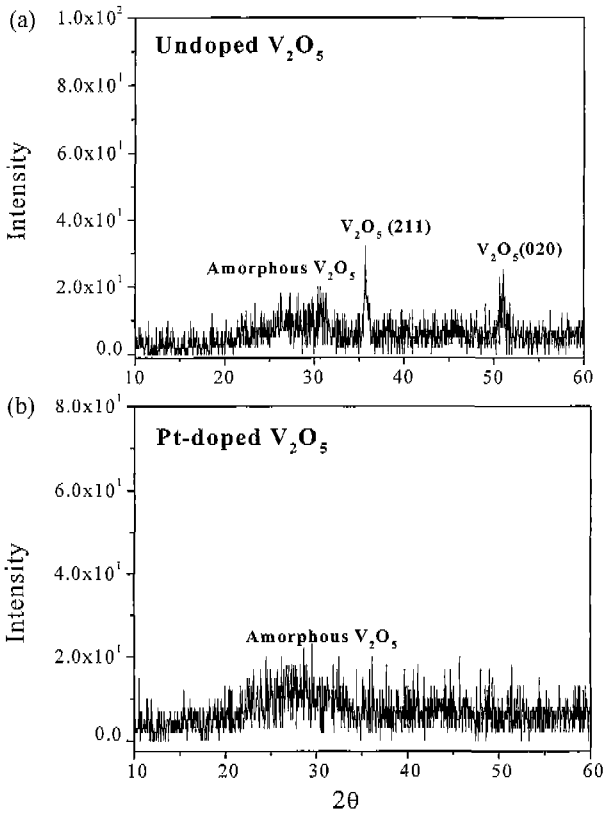

Fig. 5. X-ray diffraction plots of (a) undoped and (b) Pt-doped V_2O_5 films. It should be noted that for the 10 W-doped film, only a broad peak is seen, which is consistent with the presence of an amorphous phase.

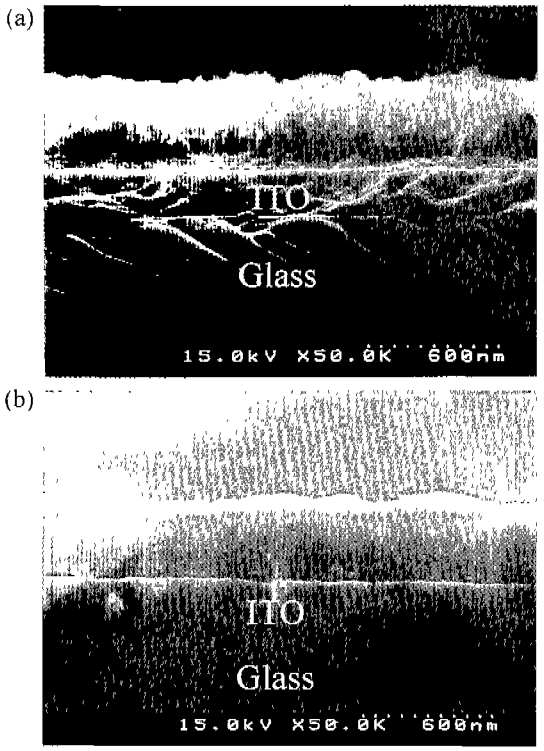

Fig. 6. SEM cross sectional images of (a) undoped V_2O_5 films and (b) a film doped at an rf power of 10W. It can be clearly seen that the Pt-doped V_2O_5 films have a denser structure and smoother surface than undoped one.

tor in deposition of a high quality LiPON electrolyte film. It is interesting to note that the thickness of the Pt-doped V_2O_5 film (400 nm) in Fig. 6(b) has changed compared to that of undoped sample(440 nm). This change in film thickness implies that the Pt doping process alters the growth kinetics of V_2O_5 films. Yu *et al.* proposed that the dopant affects the solid phase growth kinetics of amorphous alumina (Al_2O_3).[14] They concluded that the addition of Cr to amorphous Al_2O_3 decrease the growth rate, while the additions of Fe led to an increase. Because the growth kinetics of vanadium oxide film is influenced by the addition of Pt atoms, the anion and cation arrangements in oxide film would also be affected by the addition of Pt atoms. Therefore, the randomness of a Pt doped amorphous V_2O_5 film is much more than for an undoped sample, which is consistent with the XRD results.

Atomic force microscopy (AFM) was also performed, in order to investigate the surface morphology of the both undoped and Pt-doped films. As shown in Fig. 7., the Pt-doped V_2O_5 film shows a smoother morphology (rms roughness:9.2 nm) than the undoped sample(rms roughness : 19.4 nm), which is consistent with the SEM results. The smooth surface of a cathode film plays an important role in the deposition of an electrolyte film on cathode film.[15] This type of surface structure is very important in the fabrication of a TFB with a solid electrolyte thin film because the deposition of the solid electrolyte film was conducted onto this cathode film as mentioned in the experimental procedure section after growing the electrode film. For example, if defects, such as groves and/or voids, exist on the as-deposited cathode film surface, these defects will affect the surface morphology on the electrolyte film surface after the deposition of the electrolyte film on the as-deposited cathode film. That is, defects in the electrode film might led to the same types of defects on solid electrolyte film. An electron current or leakage by electrons could occur at these defects in the electrolyte film. Therefore, the growth of defect-free cathode film is very critical in achieving a high performance TFB.

The optical absorption spectra of both the undoped and th Pt-doped V_2O_5 films are shown in Fig. 8. A blank ITO/coring glass substrate was used in the reference beam in order to eliminate the substrate absorption cut-off and to compensate for any glass impurities. The fundamental absorption edge is shifted significantly from $\lambda \approx 404$ nm for undoped V_2O_5 films to $\lambda \approx 382$ nm for Pt-doped V_2O_5 films. The Shift of the maximum absorption from l^a 404 nm to l^a 382 nm suggests that the Pt doping process broadens the band gap of the V_2O_5 film. Talledo *et al.*, who investigated the CF_4 doping effect on V_2O_5 film, concluded that the excess electrons, introduced by the CF_4-doping fill the split-off band of the *d* band and increase the band gap of the V_2O_5.[16] Their explanation is consistent with our results. This similar trend

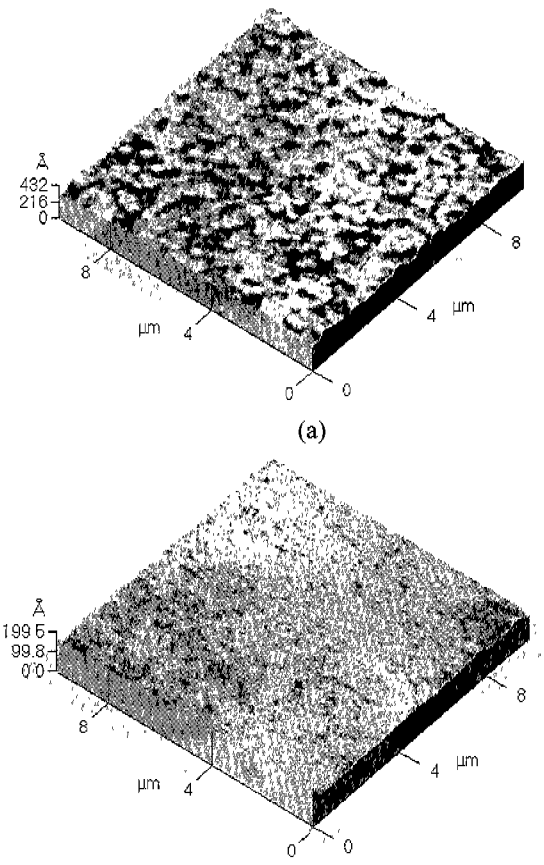

Fig. 7. AFM images of (a) undoped V_2O_5 films and (b) a film doped at a rf power of 10 W.

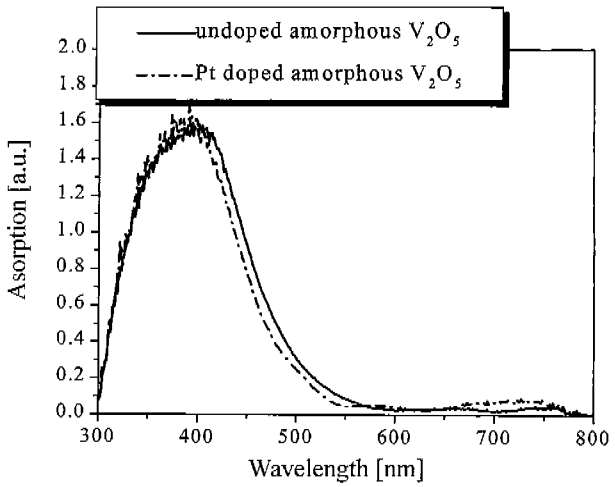

Fig. 8. Optical-absorption spectra of (a) undoped and (b) Pt-doped V_2O_5 films. It can be seen that the maximum absorption peak is blue shifted from 382 to 404 nm.

would be expected if the Pt^{6+} atoms replace the V^{5+} and the excess three electrons enter the split-off band. Fig. 9 shows the band structure model used to explain our Pt doping effect on V_2O_5 films. The broaden band edge, *i.e.*, the local-

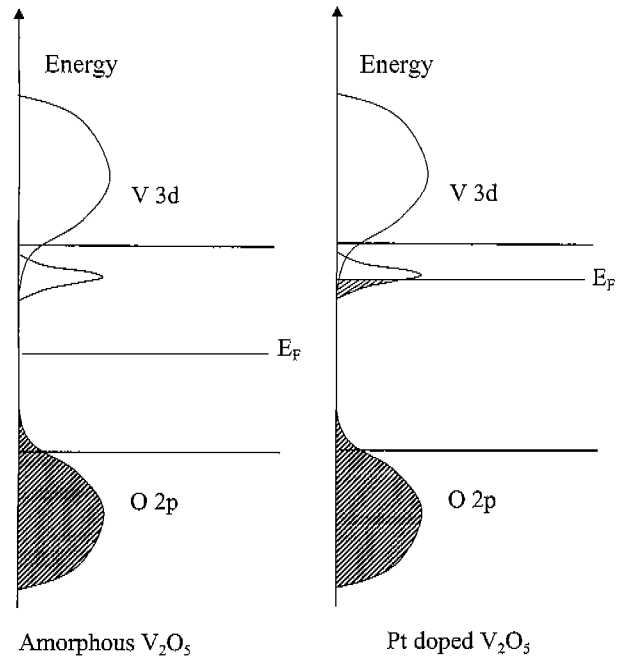

Fig. 9. A schematic band diagram used to explain optical electrical data of (a) undoped V_2O_5 films and (b) a film doped at a rf power of 10 W. The shaded region denotes filled stated in 2 O*p* and V 3*d* bands.

Table 1. A comparison of the electrical properties between the undoped and Pt-doped V_2O_5 films, as measured by Hall measurements at room temperature

	Undoped V_2O_5 film	Pt-doped V_2O_5 film
Mobility (cm^2/V-s)	25.4 (±0.2)	23.5(±0.2)
Carrier concentration (cm^{-3})	$1.69(\pm0.5)\times10^{20}$	$2.2(\pm0.5)\times10^{21}$
Bulk Resistance (Ω-cm)	1.45×10^{-3}	1.2×10^{-4}
Conductivity (/Ω-cm)	6.86×10^{2}	8.27×10^{3}

ized states, is formed as a result of increasing disorder in the Pt-doped V_2O_5 film. The region encompassed by the black line in 3p V split band of Pt-doped V_2O_5 film, indicates that excess electrons are introduced to conduction band, which can affect the carrier conduction mechanism.

To compare electrical properties between an undoped V_2O_5 film and a Pt-doped V_2O_5 film, Hall measurements were performed. Table 1. shows the results of Hall measurements both the undoped and the Pt-doped V_2O_5 film, which was measured at room temperature. Nevertheless the Pt-doped V_2O_5 films have a lower hall mobility than the undoped samples, show superior conductivity and carrier concentration, due to the effect of Pt dopant. Therefore, the improved cycle properties of Pt-doped V_2O_5 films can be explained by their superior electrical properties, which is direct result of the Pt-doping effect. As explained in the above band gap model, the excess electrons in Pt-doped V_2O_5 films might improve their electrical properties.

The Pt doping effect on the cyclic performance of V_2O_5 cathode film can be explained as follows. The XRD results showed that the small amount of Pt doping led to a completely amorphous structure with no short-range order. Because the growth kinetics of a vanadium oxide film is influenced by the addition of Pt atoms, the anion and cation arrangements in an oxide film would be affected by addition of Pt atoms. If the presence of Pt could affect the growth of the films, the modified growth behavior might be responsible for the occurrence of different microstructures. The exact reason for the doping dependence of the microstructures of the V_2O_5 films is not clearly understood at this time. Another possible Pt doping mechanism for improved cycle performance is that the Pt atom acts as a dopant in the V_2O_5 cathode film. As shown in Fig. 8., the replacement of Pt^{8+} for V^{5+} atoms leads to the excess electrons in the split off band. These excess electrons play an important role in electron conduction of the V_2O_5 cathode film. Therefore, the improved cyclibility of Pt doped V_2O_5 cathode film could be related to the combined effects of the random structure with no short-range order caused by the Pt doping process and improved electrical properties, as the result of the Pt dopant effect.

4. Summary

The Pt doping mechanism on amorphous V_2O_5 films was investigated using charge-discharge measurements, XRD, SEM, AFM and a band gap model. It was shown that the Pt-doped samples show better cycling performance than undoped ones. From the XRD results, it was found that the undoped film is amorphous with some microcrystalline phases. However, doping of the films at an rf power of 10 W resulted in completely amorphous V_2O_5. The increase of the order of amorphization is responsible for improving TFB cycle properties. In addition, the excess electrons introduced by Pt-doping process play an important role in improving the electrical properties of V_2O_5 cathode films. Therefore, the improved cyclibility of a Pt doped V_2O_5 cathode film can be related to the combined effects of the random structure with no short-range order caused by the Pt doping process and improved electrical properties, as the result of the Pt dopant effect.

Acknowledgements

This work was supported by the G7 project and the Brain Korea 21 project.

References

1. M. Baba, N. Kumagai, H. Kobayashi, O. Nakano and K. Kishidate, *Electrochemical and Solid- State Letters*, **2**, 320 (1999).
2. N. J. Dudney, J. B. Bates, R. A. Zuhr, S. Young, J. D. Robertson, H. P. Jun and S. A. Hackney, *J. Electrochem. Soc.*, **146**, 2455 (1999).
3. J. B. Bates, N. J. Dudney, B. J. Neudecker, F. X. Hart, H. P. Jun and S. A. Hackney, *J. Electrochem. Soc.*, **147**, 59 (2000).
4. H. Arai, S. Okada, H. Ohtsuka, M. Ichimura and J. Yamaki, *Solid State Ionics*, **80**, 261 (1995).
5. J. B. Bates, G. R. Gruzalski, N. J. Dudney, C. R. Luck and Xiaohua Yu, *Solid State Ionics*, **70/71**, 619 (1994).
6. Ji-Guang Zhang, Jeanne M. McGraw, John Turner and David Ginley, *J. Electrochem. Soc.*, **144**, 1630 (1997).
7. J. B. Bates, G. R. Gruzalski, N. J. Dudney, C. F. Luck, X. H. Yu and S. D. Jones, *Solid State Technology* **7**, 59 (1993).
8. H.-K. Park, W. H. Smyrl and M. D. Ward, *J. Electrochem. Soc.*, **142**, 1068 (1995).
9. F. Coustier, J. Hill, B. Owens, S. Passerini and W. Smyrl, *J. Electrochem. Soc.*, **146**, 1355 (1999).
10. H.-K. Kim, E. J. Jeon, Y.-W. Ok, T.-Y. Seong, W. I. Cho and Y. S. Yoon, *J. Electrochem. Soc.*, Submitted.
11. H.-K. Kim, E. J. Jeon, Y.-W. Ok, T.-Y. Seong, W. I. Cho and Y. S. Yoon, *Bulletin of the Korea Institute of Electrical and Electronic Material Engineering*, **13**, 751, (2000).
12. P. Aldebert, N. Baffier, N. Gharbi and J. Livage, *Mater. Res. Bull.*, **16**, 669 (1981).
13. J. Legendre and J. Livage, *J. Colloid Interface Sci.* **94**, 75 (1983).
14. Ning Yu, Todd W. Simpson, Paul C. Mclntyre, Michael Nastasi and lan V. Mitchell, *Appl. Phys. Lett.*, **67**, 924 (1995).
15. E. J. Jeon, Y. W. Shin, S. C. Nam, W. I. Cho and Y. S. Yoon, *J. Electrochem. Soc.*, (accepted for publication).
16. A. Talledo, B. Stjerna and C. G. Granqvist., Appl. Phys. Lett. **65**, 2774 (1994).